Journal of Hazardous Materials 191 (2011) 219–227

Contents lists available at ScienceDirect

Journal of Hazardous Materials

journal homepage: www.elsevier.com/locate/jhazmat

Mineralogy and leachability of gasified sewage sludge solid residues

Ana Belén Hernandez[a], Jean-Henry Ferrasse[a,*], Perrine Chaurand[b], Hans Saveyn[a,c,d], Daniel Borschneck[b], Nicolas Roche[a]

[a] M2P2, Laboratoire de Mécanique, Modélisation et Procédés Propres, CNRS-Aix-Marseille University, UMR 6181, Aix-en-Provence, France
[b] CEREGE, Centre Européen de Recherche et d'Enseignement des Géosciences de l'Environnement, CNRS-Aix-Marseille University, UMR 6635, ECCOREV, Aix-en-Provence, France
[c] Institute for Prospective Technological Studies – IPTS, Joint Research Centre (JRC), European Commission, Spain
[d] Particle and Interfacial Technology Group, Ghent University, Belgium

ARTICLE INFO

Article history:
Received 22 December 2010
Received in revised form 10 April 2011
Accepted 16 April 2011
Available online 22 April 2011

Keywords:
Waste management
Ash
Micro-XRF
Pollutants
SIMPLISMA

ABSTRACT

Gasification of sewage sludge produces combustible gases as well as tar and a solid residue as by-products. This must be taken into account when determining the optimal thermal conditions for the gasification process. In this study, the influence of temperature, heating atmosphere and residence time on the characteristics of the gasified sewage sludge residues is investigated. ICP-AES analyses reveal that the major chemical elements in the char residues are phosphorus, calcium, iron and silicon. Heavy metals such as copper, zinc, chromium, nickel and lead are also present at relatively high levels – from 50 to more than 1000 mg/kg of dry matter. The major mineral phases' identification – before and after heating – as well as their morphology and approximate chemistry (XRD and SEM-EDX) demonstrate that a number of transformations take place during gasification. These are influenced by the reactor's temperature and the oxidative degree of its internal atmosphere. The copper-, zinc- and chromium-bearing phases are studied using chemometric tools, showing that the distribution of those metals among the mineral phases is considerably different. Finally, batch-leaching tests reveal that metals retained in the residue are significantly stabilized after thermal treatment to a higher or lower extent, depending on the thermal conditions applied.

1. Introduction

About 10 million tonnes dry matter (d.m.) of sewage sludge (SS) were produced each year in the EU for the period 2003–2006 [1]. Currently, the main disposal methods are landfilling, agricultural recycling and incineration. Due to growing sludge production, landfilling cannot be considered as a sustainable approach to sludge management. Also, agricultural recycling is strongly regulated at EU level by the sludge directive, prohibiting the use of untreated sludge on agricultural land, unless it is injected or incorporated into the soil (directive 86/278/EEC) [2]. This directive also sets limit values for heavy metals and organic compounds contents – these limits are expected to be stringently reviewed in the next years. In this context, thermal conversion is an attractive way for SS disposal. This alternative, not only enables the removal of organic pollutants and pathogenic organisms, but also leads to a remarkable volume reduction of waste and allows for the recovery of the sludge energy content [3].

The most established thermal technology is incineration [4], which can provide energy by heat recovery from hot exhaust gases. Nevertheless, incineration requires two major treatment operations: extensive gas cleaning – to match the emission limit values set for air pollutants (directive 2000/76/EC) [5] – and safe disposal of ashes, containing considerable concentrations in potentially toxic metals such as Zn, Cu, Cr, Ni, Cd, Pb, As, Hg, Mo, Se and Sb [6,7]. Depending on their distribution in the incinerator, ashes present different physical characteristics and heavy metals contents and so they are classified as bottom ashes, fly ashes and slurries [8]. Over the last years increasing attention has been given to incinerated sewage sludge ashes (ISSAs) management and some studies have focused on its chemical, physical, leaching and ecotoxicological characterizations [6,8–10], phosphorus recovery [11], metals recovery [12] as well as its reuse [13].

Lately, several advanced thermal technologies have been introduced as a clear alternative to incineration [14], e.g. thermal gasification, consisting in cracking and converting the volatiles and carbon contained in the biomass at high temperatures – typically between 700 and 900 °C – and low oxidative atmosphere. The organic content of biomass is converted into combustible gases such as H_2, CO, CH_4, which after tar and ash cleaning, can be combusted to generate electricity and heat. Until now, research on SS gasification has focused on gas production yield and gas composition [3,15–21] as well as on power generation [22], but there is still a lack of knowledge on the mineralogy and leachability of the

* Corresponding author. Tel.: +33 4 42 90 85 05.
E-mail address: jean-henry.ferrasse@univ-cezanne.fr (J.-H. Ferrasse).

0304-3894/$ – see front matter © 2011 Elsevier B.V. All rights reserved.
doi:10.1016/j.jhazmat.2011.04.070

Table 1
Sewage sludge proximate analysis: average and standard deviation (in brackets) values of five repetitions.

Moisture, wt%	Volatile content, wt% d.m.	Fixed carbon, wt% d.m.	Ash content, wt% d.m.
83 (3)	63 (3)	11 (5)	32.5 (0.4)

d.m.: dry matter.

solid gasified sewage sludge residues (GSSRs), which represents approximately 30% of the solids initial dry mass [14].

The presence of heavy metals is one of the major problems related to sewage sludge and sewage sludge ashes [6,9,23–26]. For instance, if those are disposed of by landfilling, metals can be solubilized by rainwater and then leach and accumulate in topsoil or contaminate groundwater. Therefore, the European Directive 99/31/ED on landfilling [27] requires a detailed knowledge on the composition and leaching behavior of residues, in order to allow for their classification and to set compliance procedures. Research shows that metals in the SS are mainly contained in the leachable organic fractions, but heating convert them into less soluble forms [28,29]. Also, metals solubility is influenced by the oxidative degree of the atmosphere in the reactor during heating [30]: chromium is more soluble under oxidative incineration conditions than reductive pyrolysis conditions whereas copper, zinc and lead show the opposite trend. Recently, Saveyn et al. [31] examined the fate of heavy metals during gasification of SS and determined that Cu, Cr, Ni, Pb and Zn were present in the GSSR in concentrations from less than 50 mg/kg (Pb) to more than 1000 mg/kg (Cu). Since those previous works do not determine the mineralogical characteristics of residues, metals distribution among the mineral phases remains uncertain and so the study of their leaching behavior remains incomplete.

The present study deals with this lack of knowledge of the GSSR characteristics – not only essential to establish a safe final disposal for those residues, but also to determine the optimal thermal conditions for the gasification process. Hence, gasification experiments were run to investigate the influence of different operative conditions, on: 1, GSSR chemistry and mineralogy; 2, location and leaching behavior of metals concentrated on the GSSR.

2. Materials and methods

2.1. Sewage sludge samples and thermal treatment

Centrifuged SS was sampled from a municipal wastewater plant (Aix-en-Provence, France, about 200,000 p.e.). In order to avoid variations in metal contents, a large amount of well mixed sludge was sampled at once and subsequently frozen in separate portions. Elementary and proximate analyses are shown in Tables 1 and 2.

Samples (about 200 g) were placed on a metallic support, introduced in an electrically heated horizontal bench scale tubular reactor (Fig. 1) and then submitted to thermal gasification to study the effect on the residue characteristics of temperature, atmosphere, and residence time of solids at the studied temperature. Table 2 recapitulates conditions during those experiments. A heating rate of about 15 °C/min was applied until the target temperature was reached. Steam produced by a laboratory water heater was pushed by either inert gas (argon) or air to generate the corresponding heating atmospheres. The gas production yield was measured and its composition analyzed on-line by gas chromatography (GC) and Fourier transformed infra-red spectrometry (FTIR). Also, a sample of SS was dried at 105 °C for 24 h with the aim of comparing GSSR and primary dried sewage sludge (DSS).

A sufficient amount of each sample was finely crushed in an agate mortar and sampled to perform elemental analyses (CHNS), ICP-AES, XRD and μ-XRF analyses.

2.2. Characterization of residues

The chemical composition of residues (major and trace elements) was determined by ICP-AES (Horiba Ultima-C 2000), after either acid digestion by HNO_3 and H_2O_2 or alkaline hydrolysis by $LiBO_2$ [32,33]. Also C, H, N, S and O contents were measured in duplicate with an accuracy of ±0.2% using a Thermo Finnigan EA 1112.

The major mineral phases were determined with an X-ray θ–θ diffractometer (X'Pert Pro MPD, Panalytical) using Co Kα radiation (λ = 1.79 Å) and running at 40 kV and 40 mA, with a linear detector X'Celerator and a secondary flat monochromator. Samples were placed on a zero-background silicon plate and spinned at 15 rpm. A counting time of 22 s per 0.033° step was used for 2θ in the 5–80° range. The International Center of Diffraction Data PDF-2 database and the X'Pert Highscore plus software (Panalytical) were used to identify the mineral phases from the obtained X-ray diffraction (XRD) patterns.

SEM-EDX analyses were performed to examine the morphology (phase's shape and size) and chemistry of the mineral phases. Non-crushed samples were cast in Epoxy, polished and carbon-coated before being placed in the SEM (Phillips XL30 SFEG). Different areas of samples were investigated by SEM running at 20 keV and using backscattered electron images. The element distribution in GSSRA&C samples was examined by punctual analyses using EDX (5 μm diameter on 100 randomly chosen points for each sample).

The location of metals among the mineral phases was examined by more sensitive micro-analyses, using a XGT7000 spectrometer (Horiba Jobin Yvon) equipped with a Rh X-ray tube and running at 30 kV power in partial vacuum. Samples (100 mg) were pressed in the form of 13 mm diameter pellets. For each sample, μ-XRF punctual measurements (10 μm) were performed on 40 randomly chosen points during a counting time of 600 s/point. As the X-ray beam penetrated within the matrix, the obtained spectral data corresponded to the mixture of all the chemical elements detected (Mg, Al, Si, P, S, K, Ca, Ti, Cr, Fe, Cu and Zn), which constituted several mineral phases. Data was arranged in a [nm] matrix containing the intensity values for each n emission line (named variables) and for the m points analyzed. The mixture spectra matrix was treated with the SIMPLe-to-use Interactive Self-modeling Mixture Analysis algorithm (SIMPLISMA) [34]. This specific approach was previously used, with μ-XRF spectral data, to investigate the Cr- and V-bearing phases in steel slag [35] and the copper speciation in pig slurry [36]. SIMPLISMA is based on the presence of so-called pure variables – i.e. variables with a significant standard deviation of intensity for the m points. Assuming validity of the Beer Lambert law and comparing the pure variable's mean intensity with the standard deviation of the intensity for the other variables, SIMPLISMA calculates a spectrum associated with this pure variable (resolved spectrum) – formed by the elements which "vary" identically to the pure variable for the m points – and its relative weight to the mixture spectrum. Elements which "vary" identically are located together in samples and so each resolved spectrum represents the mixture of bearing phases for its pure variable. The initial spectral data can be reconstructed by the sum of the resolved spectra multiplied by the relative average weight – concentration in arbitrary units.

2.3. Leaching tests

The solubility of elements in DSS and GSSR samples was studied by a one-stage batch leaching test at a liquid to solid ratio

Table 2
Thermal conditions during gasification experiments, resulting weight loss and chemical composition of samples. Chemical data correspond to mean values and standard deviations (in brackets) calculated from two different samples obtained from the same experiment.

Sample reference	DSS[a]	GSSRA	GSSRB	GSSRC	GSSRD	GSSRE
Thermal conditions during gasification experiments						
Treatment temperature (°C)		900	700	900	900	900
Residence time (min)		30	30	30	270[b]	270[b]
Treatment atmosphere		Steam	Steam	Air/steam[c]	Air/steam[c]	Steam
Weight loss (wt% d.m.)		68.12	59.11	70.03	72.96	69.9
Elementary analysis of samples (wt% d.m.)						
C	32.40 (0.08)	4.03 (0.10)	22.32 (0.20)	1.59 (0.10)	0.12 (0.01)	0.18 (0.01)
H	5.01 (0.21)	0.13[d] (0.03)	0.77[d] (0.30)	0.22 (0.01)	0.05[d] (0.01)	0.03 (–)
N	5.19 (0.01)	0.22 (–)	1.90	(0.21) 0.28	(0.04) <0.01	<0.01
S	0.92 (0.04)	0.08 (0.01)	0.22 (0.07)	0.35 (0.01)	0.22[d] (0.05)	0.02[d] (0.01)
O[c]	28.50 (1.34)	0.52 (0.04)	5.06 (0.05)	1.90 (0.15)	0.60 (0.01)	0.34[d] (0.10)
Major elements content (wt% d.m.)						
P	4.18 (0.60)	14.13 (0.85)	10.22 (0.72)	14.33 (0.86)	14.88 (0.87)	15.19 (0.88)
Ca	4.97 (0.68)	13.48 (1.10)	11.00 (0.99)	14.78 (1.15)	13.57 (1.10)	14.77 (1.15)
Fe	3.87 (0.36)	11.82 (0.72)	8.81 (0.62)	12.11 (0.73)	12.28 (0.73)	12.42 (0.74)
Si	2.08 (0.30)	6.15 (0.71)	4.36 (0.60)	6.18 (0.71)	6.34 (0.72)	6.49 (0.73)
Mg	0.96 (0.19)	3.52 (0.40)	2.45 (0.34)	3.50 (0.40)	3.59 (0.41)	3.57 (0.40)
Al	1.01[d] (0.27)	3.07 (0.50)	2.26 (0.43)	3.03 (0.50)	3.09 (0.50)	3.24 (0.52)
K	0.30[d] (0.22)	1.12[d] (0.38)	0.76[d] (0.31)	1.07[d] (0.37)	1.14[d] (0.38)	0.98[d] (0.35)
Ti	0.16[d] (0.10)	0.56[d] (0.23)	0.43[d] (0.20)	0.56[d] (0.23)	0.57[d] (0.23)	0.56[d] (0.23)
Na	0.07[d] (0.06)	0.24 (0.08)	0.14 (0.06)	0.25 (0.09)	0.26 (0.09)	0.30 (0.09)
Mn	0.01[d] (0.02)	0.05[d] (0.03)	0.03[d] (0.02)	0.05[d] (0.03)	0.05[d] (0.03)	0.05[d] (0.03)
Trace metals content (mg/kg d.m.)						
Cu	529 (8)	1346 (6)	1159 (8)	1360 (9)	1367 (5)	1494 (10)
Zn	423 (10)	757 (4)	753 (5)	854 (5)	877 (4)	702 (6)
Cr	36 (7)	104 (2)	98(1)	244[e](3)	633[e] (4)	137 (3)
Ni	66 (2)	165 (4)	122(1)	141[e](3)	116[e] (2)	122 (3)
Pb	45 (4)	51 (1)	88 (1)	89 (2)	90 (1)	48 (1)
Cd	1 (–)	<LOD	<LOD	<LOD	<LOD	<LOD
Hg	2 (–)	<LOD	<LOD	<LOD	<LOD	<LOD

d.m.: dry matter; LOD: limits of detection.
(–) Non-significant value. Weight loss was calculated as follows: weight loss [%] = $(m_0 - f/m_0) \times 100$ m_0: initial dry mass of the sample; m_f: mass of solid residue after thermal treatment.

[a] Dried sewage sludge.
[b] If 270 min is not in the typical range for industrial gasifiers, this long time assure the high conversion of residues.
[c] Air to steam ratio: 1 mol/mol (3.6 mol/h); organic oxygen content.
[d] Relative standard deviation bigger than 20%.
[e] Samples polluted by the Cr-Ni alloy support.

of 10. Such tests, rather simple to perform, give an initial indication on the residues' stability and allow the comparison between them. A rotary device (10 rpm) stirred the residues (4.5 g) in contact with ultrapure water (45 ml) during one month. Leachates samples (10.5 ml) collected after 24 h, 6 days and 30 days were filtered at 0.45 μm, acidified and analyzed by ICP-AES. After leachate sampling, ultrapure water (10.5 ml) was added to keep the liquid to solid ratio constant. Tests were carried out in duplicate and control tests were performed at the same time. The conductivity and pH were also monitored during the experiment.

3. Results and discussion

3.1. Chemical composition

Gasification of sludge samples at 700 °C (GSSRB) and 900 °C (GSSRA&C&D&E) resulted in a mass reduction of between 60 and 70% (d.m.), respectively (Table 2). Thermal conversion of organic matter contained in the sludge, to form principally H_2, CO, CO_2, CH_4, C_xH_y, NH_3, COS – according to FTIR and CG analyses – and tar, implied losses on C, H, N, S and O content. Temperature was the main parameter controlling those losses: 28% of initial carbon con-

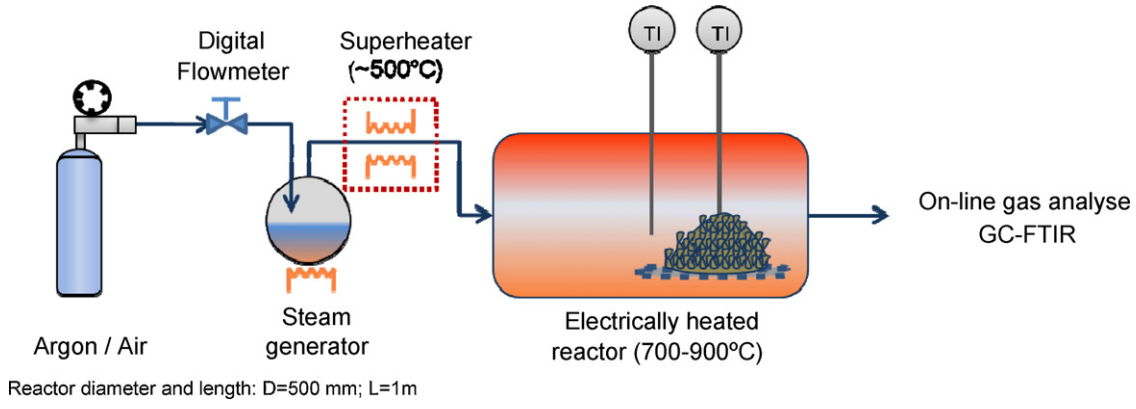

Fig. 1. Experimental setup schema.

tent remained in the GSSRB (700 °C), while less than 4% was still present in the GSSRA&C&D&E (900 °C). Sulfur volatilization and air presence were also related: more than 11 and 6% of initial sulfur content remained in GSSRC&D (air-steam) whereas less than 3 and 1% remained in GSSRA&E (steam). Nitrogen was mostly removed for solids undergoing long time treatments (GSSRD&E, 270 min).

Metal contents of SS may widely vary, depending on the sludge's origin. The SS used in this work had similar metal contents that values found in literature [14], so it can be considered as representative. Only cadmium, chromium and lead exhibited values in the lower typical range (<10, <500 and <500 mg/kg, respectively).

During gasification, the major elements measured by ICP-AES were concentrated on the GSSR, because of the residues weight loss. Actually, data obtained for GSSR when represented according to their initial mass in SS revealed that elements such as P, Ca, Fe, Si, Mg, Al, K, Ti, Na, Mn were nearly all retained in the char and their contents in GSSRA&C&D&E (900 °C) were rather similar.

Heavy metals showed different retrieval ratios in the GSSR [31]: between 70 and 90% of copper, less than 80% of lead and between 50 and 65% of zinc initial contents were recovered in the GSSR. Cadmium and mercury were highly volatilized. Heavy metals vaporization is known to increase with temperature and depend on the matrix composition [37]. Concerning chromium and nickel, GSSRC&D samples were contaminated by the metal support foam, which consisted of a nickel–chromium alloy and so values measured for those samples were inconsistent (chromium seemed to be retrieved on those samples at ratios over 100%).

Because of their potential toxicity and their high concentration levels, special attention has to be given to copper, zinc (>1000 and 700 mg/kg of d.m., respectively), chromium and nickel (>100 mg/kg of d.m. in GSSRA&B&E samples) retained in the GSSR. The solubility of those metals, which strongly depends on their speciation, is discussed in Section 3.4.

3.2. Mineralogy

3.2.1. XRD measurements

Quartz (SiO_2), calcite ($CaCO_3$) and vivianite ($Fe_3(PO_4)_2{\cdot}8H_2O$) were the main crystalline phases identified in the DSS (Fig. 2). Vivianite is known to precipitate in the sludge as a consequence of SS treatment (coagulant addition, digestion, dewatering, reducing conditions) [38]. Also, a low intensity peak at 3.25 Å (31.9° Co Kα 2θ), corresponding to the rutile (TiO_2) major peak, was observed – according to ICP-AES data, TiO_2 mass content (if it is considered that all the major elements are in their oxide form) is about 0.25% in the DSS and 0.9% in the GSSR. No other minerals were correctly identified but the presence of low intensity peaks at 14, 7, 4.7 and 3.5 Å may indicate the presence of a clay mineral belonging to the chlorites family.

The XRD data for DSS presented a slightly raised background between 20° and 40° (Co Kα 2θ), which indicates the presence of an amorphous phase. This amorphous phase could not be characterized, however it seemed to be rich in organic matter (see C, H, N, S and O contents in Table 2) and rich in phosphorus since the ICP-AES data showed an atomic excess of P to Fe (2:1) and the only mineral phase identified containing phosphorus was vivianite, whose atomic ratio P to Fe is 2:3. After heating at 700 °C (GSSRB), the amorphous phase was present in the residue in a lower extent and it disappeared at 900 °C (GSSRA&C&D&E). This can be explained by the organic matter volatilization (Table 1) and the amorphous mineral matter crystallization.

Regarding the thermal stability of mineral phases, quartz (31° (Co Kα 2θ)) and rutile remained stable, whereas calcite and vivianite decomposed during gasification to form new mineral phases. Actually, calcite peaks were detected in the GSSRB (following 700 °C steam treatment) but their intensity was strongly reduced when compared with quartz peaks. Thermal decomposition of calcite, at about 850 °C, is known to form limestone and gaseous carbon dioxide, according to the reaction: $CaCO_3(s) \rightarrow CaO(s) + CO_2(g)$, which can be catalyzed by steam [39]. The decarbonation process is almost completed at 950 °C [40] and calcite intensity peaks on samples treated at 900 °C (GSSRA&C&D&E) were indeed drastically reduced. Limestone – in its hydrated form, portlandite ($Ca(OH)_2$ – was only detected on GSSRB (700°), therefore limestone, at higher temperature, seems to react with other species to form new compounds.

Vivianite completely disappeared at temperatures below 700 °C. A thermal study of this iron (II) mineral [41] has shown that its dehydration to form graftonite ($Fe_3(PO_4)_2$) is completed at 450 °C. At higher temperature, iron oxidation takes place and above 625 °C iron (III) ortho phosphate ($FePO_4$) has been identified among the thermal products [42]. During the present study, in order to better understand vivianite transformations under steam atmosphere, a 2 g sample of vivianite was put into the oven, submitted to the same gasifying conditions as GSSRA and analyzed by XRD. The formed compound patterns corresponded to graftonite ($Fe_3(PO_4)_2$) suggesting that despite the high temperatures, after 30 min of steam gasification, dehydration occurred without iron oxidation.

The new peaks, appearing after gasification, were identified as whitlockite ($Ca^{2+}{}_{18.19}(Mg^{2+}{}_{1.17}, Fe^{2+}{}_{0.83})H_{1.62}(PO_4)_{14}$), stanfieldite ($Ca^{2+}{}_4(Mg^{2+}, Fe^{2+})_5(PO_4)_6$), hematite ($Fe^{3+}{}_2O_3$) and farringtonite ($Mg_3(PO_4)_2$). Those new peaks become more intense and narrow with increasing temperature, meaning that those minerals were better crystallized. Whitlockite, quartz and hematite are commonly found in ISSA [6,43]. Portlandite, limestone, anhydrite ($CaSO_4$) and aluminum phosphate ($AlPO_4$) were also found when P-bioavailability on ISSA was investigated [11]. However stanfieldite and farringtonite presence in ISSA is not reported in literature and so they seem to be distinctive of the GSSR.

Iron appeared to be incorporated in different minerals. However iron (II) was only associated to Ca-, Fe- and Mg-phosphates while iron (III) was only associated to hematite. It turned out that the formation of hematite and stanfieldite was clearly influenced by the oxidative degree of the heating atmosphere. When only steam was introduced in the reactor (GSSRA&B&E), hematite was not present, whereas after air-steam gasification (GSSRC&D) hematite was formed and the intensity of stanfieldite peaks was significantly reduced. Concordantly, the reddish color characteristic of hematite was only observed on GSSRC&D samples (GSSRA&B&E samples presented different shades of grey). The absence of hematite in GSSRA&B&E samples can be explained by similar mechanisms which take place in blast furnaces during iron ore reduction by CO and H_2 – both produced during SS gasification – at about 580 °C, to form metallic iron [44,45]. Metallic iron, during air-steam experiments (GSSRC&D), is supposed to be oxidized to form hematite.

In general, the identified mineral phases seemed to form solid solutions (having variable chemistry) and contained different elements as impurities since detected peaks were slightly shifted and their relative intensity altered. For instance, whitlockite is a calcium phosphate able to contain Mg and Fe in variable proportions and depending on its chemical composition the relative intensity and position of peaks slightly varies. To examine the chemistry of mineral phases SEM-EDX punctual measurements were performed.

3.2.2. SEM-EDX analyses

SEM pictures of DSS (Fig. 3a) presented grains of very irregular shape and size embodied in a compact and darker structure (containing lighter elements). Chemical analyses were performed on the brighter grains (heavier elements), belonging to: calcite, quartz, phosphates containing variable amounts of Ca, Fe and Mg, and silicates containing variable amounts of Al, Na, K, Fe, Ca and Mg.

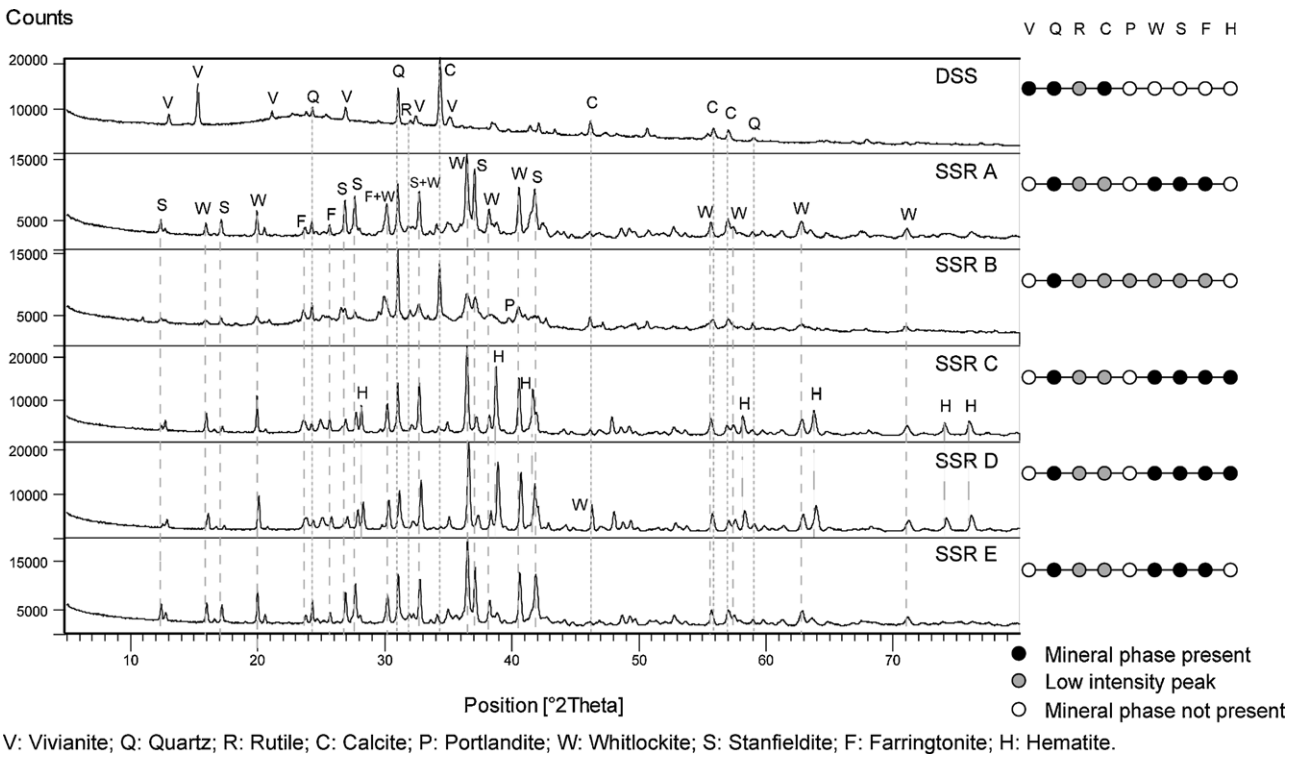

Fig. 2. XRD patterns of DSS and GSSRA&B&C&D&E.

GSSR samples also contained irregular grains; yet the surrounding structure was much more porous (Fig. 3b–d). The biggest dark-grey grains corresponded mainly to quartz grains, whereas the amorphous porous structure around was mostly formed by Ca, Fe and Mg-phosphates – the brightest areas in this structure corresponded in general to iron-rich phosphates. Besides, small bright grains embodied in those phosphates appeared when SS was treated with air-steam (Fig. 3c and d). The EDX-analyses of those points revealed a high iron content, and therefore they are supposed to correspond to hematite – detected by XRD.

Punctual chemical analyses performed on GSSRA&C, revealed the presence of Al-K-silicate – possibly feldspar $KAlSi_3O_8$, Mg-silicate, Al-phosphate and Fe-phosphate – possibly graftonite, $Fe_3(PO_4)_2$ – together with the mineral phases previously detected by XRD (calcite, whitlockite, stanfieldite, farringtonite, hematite and quartz). Most of the chemical analyses corresponded to the combination of several mineral phases since the grain size was frequently smaller than the spots analyzed (5 μm). The chemical composition of phosphates presented variable amounts of Ca, Fe and Mg (Fig. 4). A large amount of points were plotted

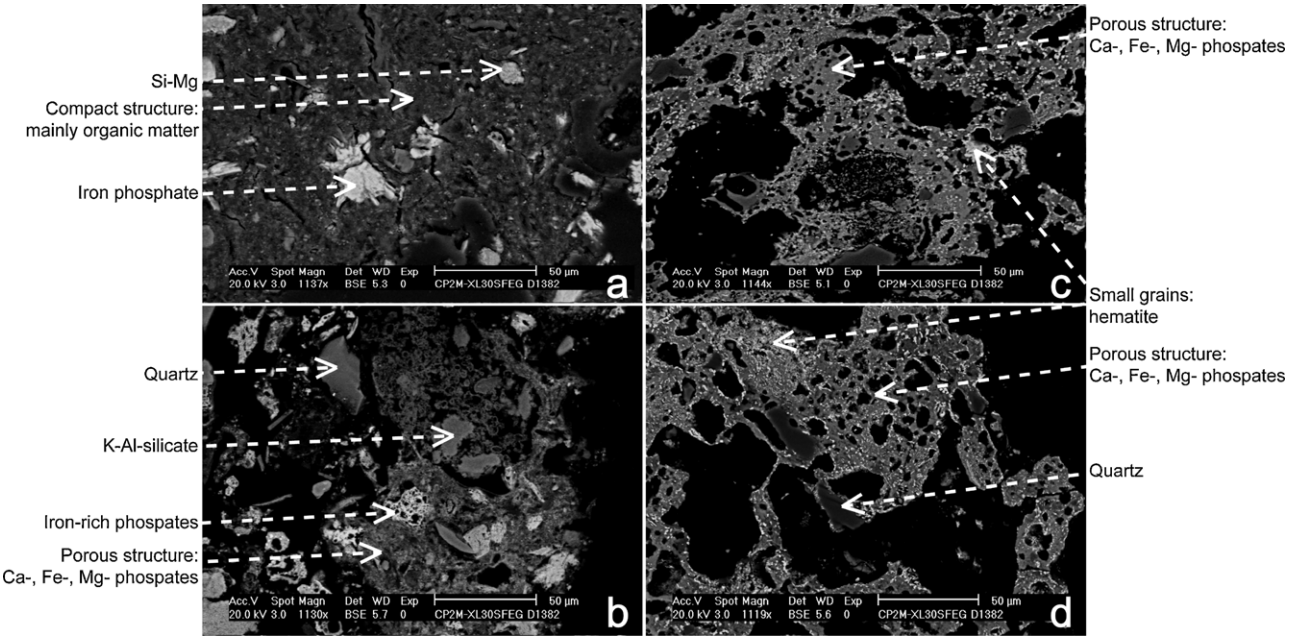

Fig. 3. SEM pictures of DSS (a), GSSRA (b), GSSRC (c) and GSSRD (d). White arrows point out some of the mineral phases typically found in samples.

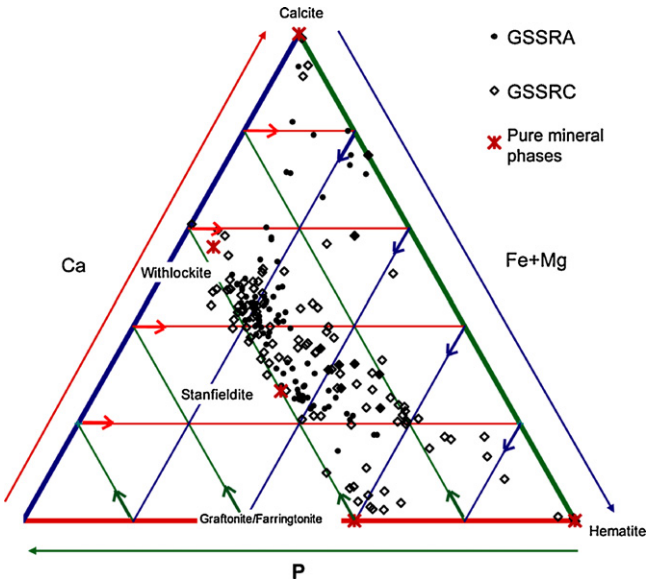

Fig. 4. Phosphates distribution in the Ca, P and Fe + Mg ternary diagram. Points containing higher amounts of Si than P or Ca or Fe were not represented.

between whitlockite and stanfieldite – solid solution with variable amounts of each compound. Concordantly with XRD results, air-steam gasification seems to form iron-richer phosphates than steam gasification, as it can be observed in Fig. 4 – points represented in the bottom right corner corresponded to the combination of hematite with stanfieldite or whitlockite. Also, the vicinity of those phases may confirm the oxidation of iron coming from the iron phosphates as discussed in the previous section.

3.3. Heavy metals distribution

Copper, zinc and chromium were correctly isolated by SIMPLISMA in their corresponding resolved spectra, meaning that their distribution among the mineral phases was different – which implies different bearing phases. The intensity of the peak for each element (Mg, Al, Si, K, P, Ca Ti and Fe) – identified by their energy emission lines – in the Cu-, Zn- and Cr-resolved spectra was multiplied by the corresponding average weight to determine the elements distribution among the resolved spectra. This distribution – together with the chemical composition of samples – was used to calculate the chemical average composition of the mixture of bearing phases (Fig. 5). Mole contents were calculated using the phosphorus mole content (element moles over phosphorous moles), since phosphorus was the major element in GSSR and it constituted many major mineral phases. The identification of each metal-bearing phase in the mixture was complicated given the residues' intricacy – i.e. too many elements arranged in several mineral phases. Hence, various chemical data sets were compared. As such, the chemical compositions of the metal bearing phases were compared side by side, and also with the total average sample composition (reference values). These comparisons highlighted that certain elements were remarkably only abundant in the associated resolved spectrum of the metal bearing phases, which allowed them to be easily mapped out on the sample. The total sample's chemical composition – discussed in Section 3.1 and further used as reference value – was nearly the same for the GSSRA&C&D&E, the average chemical composition expressed per mol of P being: 0.31 Mg, 0.24 Al, 0.48 Si, 0.06 K, 0.75 Ca, 0.02 Ti and 0.46 Fe.

Results showed that copper was mainly located in Ca-rich regions since calcium content was much higher in the average Cu-bearing phase than in the total residue (reference values). The ratio

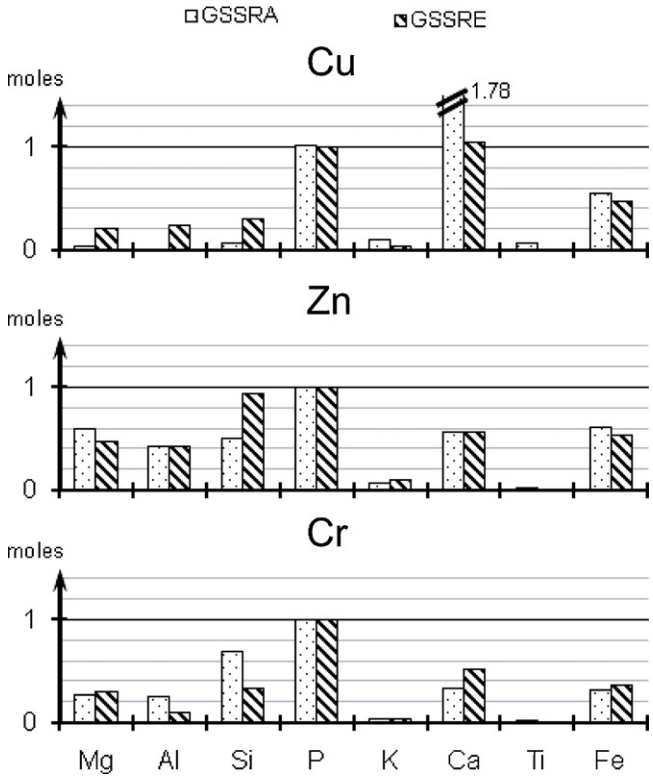

Fig. 5. Chemical composition (moles/P moles) of the mixture of bearing phases for copper, zinc and chromium according to the SIMPLISMA resolved spectrums.

of Ca to P in the average Cu-bearing phase for GSSRA&E was 1.04 and 1.78, respectively; therefore whitlockite – Ca to P ratio of 1.5 – was pointed out as the main Cu-bearing phase in those samples.

Concerning zinc, its average bearing phase showed Mg, Al, Si and Fe contents above the reference. Those elements, according to XRD and SEM-EDX results, formed farringtonite, graftonite, Mg- and Al-K-silicates.

Finally, average Cr-bearing phases showed lower contents than the reference for all the studied elements – except for silicon in GSSRA. Since mole contents were given relative to the mole content of phosphorous, this means that chromium was mostly adjacent to phosphorous – and silicon for GSSRA.

3.4. Leaching behavior

The solubility of metals, which depends on their speciation, was studied in order to assess the potential hazard of residues. Table 3 shows average data obtained from duplicated leaching tests. Calcium and potassium were the major species released for most of the samples. Exact potassium values could not be calculated since they often exceeded the largest reference from the calibration standard series by a factor of 10 or more. Aluminum was also considerably released from most of GSSR samples: more than 7% of its initial content was measured on leachates of GSSRB, and more than 2% on GSSRA&D.

Equilibrium pHs in sample leachates (values measured the 30th day) were different depending on the thermal conditions: GSSRA&B&E (steam, 700&900 °C) were considerably alkaline over 10, GSSRD&C (air-steam, 900 °C) presented lower pH values about 7.7 and 8.8 and DSS leachates presented the lowest values about 6.4. The pH during leaching test influences the solubility of species; phosphates, for instance, are known to be stable under alkaline conditions. Conductivity values were between 0.38 and 5.16 mS/cm the 30th day. GSSRA conductivity values diminished and DSS val-

Table 3
Measured parameters during leaching tests and released amounts of constituents after 24 h, 6 and 30 days.

	Initially measured		Measured after 1, 6 and 30 days			A [mg/kg of solids DM]									
	pH	Cond. (mS/cm)	Days	pH	Cond. (mS/cm)	Al	Ca	Cr	Cu	Fe	Mg	Na	Ni	P	Si
DSS	5.48	0.86	1	6.00	d.p.	18.36	557.01	8.98	16.34	11.55	60.04	91.60	3.44	1475.58	90.68
			6	6.49	1.46	22.57[b]	1022.07	2.94[b]	7.87	23.23	96.59	308.70	3.20	1667.04	169.06
			30	6.36	5.16	16.10	955.95	1.55	1.95[b]	66.47	50.99	194.35	1.46[d]	1471.05	176.78
GSSRA	11.70	1.02	1	12.29	d.p.	98.07	2689.44	0.04[a]	2.08	0.10[b]	0.91[d]	9.61[b]	0.01	1.75[b]	11.26
			6	11.95	1.38	138.59	2162.97[c]	<0.01	1.08	0.56[b]	1.14[d]	21.88	<0.01	1.99[b]	17.45
			30	10.62	0.38	68.27	854.52	0.02[a]	0.35[b]	0.36[a]	6.67	48.27	<0.01	1.08[a]	36.01
GSSRB	11.52	1.01	1	12.07	d.p.	159.14	2321.46	0.06[a]	0.49	0.54[d]	0.44[d]	7.38[b]	0.04[a]	1.41[b]	19.87
			6	11.35	0.55	302.35[b]	1553.46	<0.01	<0.01	0.53[b]	1.41[d]	15.94	<0.01	2.38[b]	29.37
			30	10.31	0.50	240.16	1086.23	<0.01	0.10[b]	0.28[a]	11.01	31.91	<0.01	2.69[b]	24.16
GSSRC	8.00	0.50	1	7.92	d.p.	29.70	2154.09	0.93	2.87	2.35	33.55	60.24	14.68	17.62	28.77
			6	7.84	0.86	35.60	2610.14[c]	0.54	2.93	3.31	34.62	120.49	14.61	46.47	95.44
			30	7.74	1.14	31.18	2658.44[c]	0.62	3.55	2.82[d]	33.16	112.72	12.19	80.12	217.01
GSSRD	8.01	0.09	1	11.44	d.p.	68.86	2053.50	4.71	0.16[b]	<0.01	1.60[d]	7.55[b]	0.12[a]	0.68[a]	30.72
			6	9.71	0.69	128.23	2329.43[c]	6.91	<0.01	0.22[a]	27.60	23.52	<0.01	2.25[b]	11.36
			30	8.84	0.74	58.07	1697.03[c]	6.36	0.04[a]	0.16[a]	31.55	33.30	<0.01	6.22[d]	12.32
GSSRE	5.54	0.4	1	10.45	d.p.	33.83	943.75	0.22[b]	0.17[b]	<0.01	18.01	14.53	0.24[b]	1.03[b]	40.00
			6	11.41	0.36	51.49	1100.51	0.06[a]	0.11[a]	0.26[a]	9.22	33.34	0.04[a]	0.85[a]	50.87
			30	10.86	0.46	26.82	756.09	0.09[b]	0.12[b]	0.20[a]	15.66	49.34	0.04[a]	0.76[a]	96.01

d.m.: dry matter; d.p.: damaged probe Values were calculated as follows: A [mg/kg solids d.m.] = $C \times L/s = C \times 10$, C: concentration (mg/l) of a particular constituent in the leachates collected after 24 h, 6 and 30 days. L/S: liquid to solid ratio (10 l/kg).

[a] Value under limits of detection.
[b] Value under limits of quantification.
[c] Value out of range (10 times higher than highest standard).
[d] Value under 5 × value obtained during the control experiment.

ues greatly increased from the 6th to the 30th day. The high values measured for DSS conductivity are related to salts dissolved during tests – which can be associated to the lower pH. Also, the decrease in conductivity for GSSRA can be explained by the precipitation of secondary phases formed after primary phases' alteration. Finally, residence time also affect the leachability of GSSR – initial and 1st day values show significant differences – however equilibrium values for GSSRA&GSSRE and for GSSRC&GSSRD were rather similar and more tests should be performed to correctly explain the influence of this variable.

Heavy metals contained in DSS were greatly mobilized. After 24 h, 897 μg/l of chromium was leached which represents about 25% of its total content in the solid. Also nickel and copper were released in a considerable extent, about 5 and 3%, respectively.

This considerable mobility of heavy metals was highly reduced after gasification. For instance, after 24 h dissolved amounts of chromium and copper on GSSR samples were below 0.8 and 0.3% of their content in solids, respectively. Nickel was not detected for most GSSR samples, except for GSSRC, with about 10% of nickel released. The higher nickel's release can be explained by a different speciation, however it should be noted that the measured pH was less alkaline for this residue and that other elements such as Fe, Mg, P and Na were also more released for GSSRC than for the other samples.

Temperature and residence time were the main parameters influencing copper release. Increasing temperature, from 700 to 900 °C (GSSRB&A), resulted in a 3 times larger copper leachability – from 0.05 to 0.15% of copper residues content (leachates collected after 24 h). Concerning residence time, copper solubility was even lower after longer treatments – for both steam and air-steam treatments, which means that the behavior of this metal during gasification is restricted by time.

Chromium leachability was principally influenced by both heating atmosphere and residence time. While the chromium measured (after 24 h) in the GSSRA&B&E (steam) leachates was under LOD, about 90 μg/l of chromium were released from GSSRC (air-steam) and this value increased, for GSSRD, to more than 470 μg/l as a consequence of the longer thermal treatment. The higher chromium contents in GSSRD&C leachates are not believed to be a consequence of Cr-Ni metallic foam pollution since metallic chromium is not soluble under the given test conditions and the leachates were filtered before acidifying and analyzing. The higher solubility of chromium for air-steam treated residues can be explained by the oxidation of trivalent chromium to its hexavalent form – for longer treatment this oxidation is completed or almost completed. Chromium oxidation was also observed by Wang et al. [46] after MSWI fly ash (spiked with Cr_2O_3) sintering in different atmospheres (air, N_2 and $5\%H_2 + 95\%N_2$). It was also found that chromium content in the leachate is nearly duplicated when sintering time is multiplied by a factor 2 – from 30 to 60 min. Additionally, Kirk et al. [47] showed that, during thermal treatment of MSWI ash, the presence of limestone (CaO) greatly increases the leachability of chromium – by about 54% – which chemical speciation changes from Cr_2O_3 to $CaCrO_4$.

Comparison between leachability of GSSR data and other thermal residue data available in literature (Table 4) showed that the values obtained in this study were in the same range as those obtained for ISSA [6,8] and pyrolyzed sewage sludge residues [30]. Literature data correspond to leaching tests performed following the European 12457-2:2002 method and the Japanese JLT-13 method, which are performed under similar conditions – batch test, distilled water, temperature and solid to liquid ratio. Such tests should be treated as an initial indication until longer-term baseline behavior is evaluated (tests under controlled pH, long-term tests, dynamic tests, etc.). However, from this comparison it can be retained that the lowest values for copper (0.01%) were obtained after long time air-steam and steam gasification. Chromium release was between 0.04 and 0.74% – the lower values corresponded to pyrolysis and steam gasification (GSSRA), while the higher releases corresponded to incineration (Second cyclone ISSA (A)) and long time air-steam gasification (GSSRD). Yet, the comparison of residues following different thermal technologies should be completed by more tests performed on the same sewage sludge sample, to avoid variations in initial metal contents. Finally, in view of those initial results, thermal treatment performed on GSSRB&E seemed to be the best compromises dealing with cop-

Table 4
Comparison of the metal release ratios determined in this work and the metal release ratios for SS and other thermal residues found in literature.

Sample description	pH	% Released of metals				Time	Standard test	Reference
		Cu	Cr	Fe	Al			
Sewage sludge								
DSS	6.0	3.09	24.94	0.03	1.85	24 h	EN 12457-2 rescaled	this work
SS[a]	6.3	62.60	2.70			6 h	JLT-13 (Japan)	Hwang et al. [30]
Incinerated sewage sludge ash								
Bottom ISSA (assay A)[a]	10.1			0.01	0.12	24 h	EN 12457-2	Lapa et al. [8]
First cyclone ISSA (assay A)[a]	11.2		0.37		0.06	24 h		
Second cyclone ISSA (assay A)[a]	8.4		0.74		0.01	24 h		
Second cyclone ISSA (assay B)[a]	8.0		0.30			24 h		
SI[a]	11.0	0.04	0.4			6 h	JLT-13 (Japan)	Hwang et al. [30]
Pyrolysed sewage sludge residue								
SP[a]	7.9	0.1	0.04			6 h	JLT-13 (Japan)	Hwang et al. [30]
Gasification sewage sludge residue								
GSSRA (steam 900 °C 30 min)	12.3	0.15	0.04	<0.001	3.19	24 h	EN 12457-2 rescaled	This work
GSSRB (steam 700 °C30 min)	12.1	0.04	0.06	<0.001	7.04	24 h		
GSSRC (air/steam 900 °C 30 min)	7.9	0.21	>0.38[b]	<0.001	0.98	24 h		
GSSRD (air/steam 900 °C 270 min)	11.4	0.01	>0.74[b]	<0.001	2.23	24 h		
GSSRE (steam 900 °C 270 min)	10.4	0.01	0.16	<0.001	1.04	24 h		

[a] Data from literature was used to calculate the metals leaching ratios as follows: metal leaching ratio (%) = leaching concentration (mg/l)/metal content in solids (mg/kg) × 10(*L*/*S*) × 10.
[b] Since the measured Cr content in GSSRC&D samples was highly atypical given release values are underestimated.

per and chromium solubility, and that such result would therefore point out gasification as a promising alternative in SS thermal treatment.

4. Conclusions

In this study, the characteristics of the gasified sewage sludge residues (mineralogy and leaching behavior) have been studied in view of determining the optimal conditions during gasification and to establish a safe final disposal for those residues. The effects of temperature (700 and 900 °C), gasifying atmosphere (steam and air-steam) and residence time (30 and 270 min) on the sewage sludge gasification residue have been investigated. For the first time – to the authors' knowledge – chemical and mineralogical compositions of those residues have been determined by the combination of ICP-AES, XRD and SEM-EDX analyses. Also, the location of metals in the residues has been examined by μ-XRF measurements coupled with an original chemometric tool (SIMPLISMA). Lastly, the potential hazard of solids has been studied in a first approach – at laboratory scale – which allowed the comparison of those residues with incineration and pyrolysis residues. From this initial study, a number of conclusions can be drawn:

- The solid residue following sewage sludge gasification contains mainly phosphorous, calcium, iron, magnesium and silicon in the form of phosphates (Ca, Fe, Mg), quartz, silicates and oxides (Fe).
- Sewage sludge mineralogy suffers significant transformations during gasification indicated by the recrystallization of the mineral phases. The final mineralogy depends on the temperature – degree of crystallization and the heating atmosphere – oxides formation.
- The mixture of those mineral phases is highly irregular and complex (many elements arranged in different mineral phases as well as variable chemistry and irregular morphology of those mineral phases).
- Heavy metals such as copper, chromium and zinc are concentrated in those residues to relatively high levels (>100 mg/kg). Those metals are differently distributed among the mineral phases of residues.
- Thermal treatment significantly stabilizes heavy metals contained in sewage sludge. The efficiency of this stabilization depends on the metal considered and on the operative conditions applied:
  - Copper is less mobilized at 700 °C than at 900 °C. Longer residence times, at 900 °C, also stabilize copper significantly.
  - Chromium solubility increases when more oxidizing conditions and longer residence times are applied.

Finally, a comparison between thermal sewage sludge residues' leachability shows that gasification is an attractive alternative for landfilling, incineration or pyrolysis as sewage sludge disposal route in view of the solubility of heavy metals retained in the residues.

Acknowledgments

The authors would like to thank the Research Federation ECCOREV for partially financing this work, as well as Ms. Hélène Miche for technical assistance with the ICP-AES analyses. Ana Belén Hernandez would also like to acknowledge a scholarship from the French Minister of Education and Hans Saveyn a research grant from the Research Foundation Flanders (FWO) and the University Paul Cézanne.

Appendix A. Supplementary data

Supplementary data associated with this article can be found, in the online version, at doi:10.1016/j.jhazmat.2011.04.070.

References

[1] Milieu Ltd., WRc, Environmental, economic and social impacts of the sewage sludge on land. Draft Summary Report 1: Assessment of Existing Knowledge, Report for the European Commission (2009).
[2] Council Directive 86/278/EEC of 12 June 1986 on the protection of the environment, and in particular of the soil, when sewage sludge is used in agriculture.
[3] J.-H. Ferrasse, I. Seyssiecq, N. Roche, Thermal gasification: a feasible solution for sewage sludge valorisation? Chem. Eng. Technol. 26 (2003) 941–945.
[4] J. Werther, T. Ogada, Sewage sludge combustion, Progr. Energy Combust. Sci. 25 (1999) 55–116.
[5] Council Directive 2000/76/EC on the incineration of waste (the WI Directive).
[6] S. Donatello, M. Tyrer, C.R. Cheeseman, EU landfill waste acceptance criteria and EU Hazardous Waste Directive compliance testing of incinerated sewage sludge ash, Waste Manage. 30 (2010) 63–71.
[7] M. Hartman, M. Pohorely, O. Trnka, Behaviour of inorganic constituents of municipal sewage sludge during fluidized-bed combustion, Chem. Papers 61 (2007) 181–185.

[8] N. Lapa, R. Barbosa, M.H. Lopes, B. Mendes, P. Abelha, I. Gulyurtlu, J. Santos Oliveira, Chemical and ecotoxicological characterization of ashes obtained from sewage sludge combustion in a fluidised-bed reactor, J. Hazard. Mater. 147 (2007) 175–183.
[9] G. Ahlberg, O. Gustafsson, P. Wedel, Leaching of metals from sewage sludge during one year and their relationship to particle size, Environ. Pollut. 144 (2006) 545–553.
[10] C.R. Cheeseman, G.S. Virdi, Properties and microstructure of lightweight aggregate produced from sintered sewage sludge ash, Resour. Conserv. Recycl. 45 (2005) 18–30.
[11] C. Adam, B. Peplinski, M. Michaelis, G. Kley, F.G. Simon, Thermochemical treatment of sewage sludge ashes for phosphorus recovery, Waste Manage. 29 (2009) 1122–1128.
[12] K. Karlfeldt Fedje, C. Ekberg, G. Skarnemark, B.-M. Steenari, Removal of hazardous metals from MSW fly ash—an evaluation of ash leaching methods, J. Hazard. Mater. 173 (2010) 310–317.
[13] P. Garcés, M. Pérez Carrión, E. García-Alcocel, J. Payá, J. Monzó, M.V. Borrachero, Mechanical and physical properties of cement blended with sewage sludge ash, Waste Manage. 28 (2008) 2495–2502.
[14] D. Fytili, A. Zabaniotou, Utilization of sewage sludge in EU application of old and new methods—a review, Renew. Sustain. Energy Rev. 12 (2008) 116–140.
[15] A. Adegoroye, N. Paterson, X. Li, T. Morgan, A.A. Herod, D.R. Dugwell, R. Kandiyoti, The characterization of tars produced during the gasification of sewage sludge in a spouted bed reactor, Fuel 83 (2004) 1949–1960.
[16] J.J. Manyà, J.L. Sánchez, J. Ábrego, A. Gonzalo, J. Arauzo, Influence of gas residence time and air ratio on the air gasification of dried sewage sludge in a bubbling fluidised bed, Fuel 85 (2006) 2027–2033.
[17] J.J. Manyà, J.L. Sanchez, A. Gonzalo, J. Arauzo, Air Gasification of dried sewage sludge in a fluidized bed: effect of the operating conditions and in-bed use of alumina, Energy Fuels 19 (2005) 629–636.
[18] A. Midilli, M. Dogru, G. Akay, C.R. Howarth, Hydrogen production from sewage sludge via a fixed bed gasifier product gas, Int. Hydrogen Energy J. 27 (2002) 1035–1041.
[19] A. Midilli, M. Dogru, C.R. Howarth, M.J. Ling, T. Ayhan, Combustible gas production from sewage sludge with a downdraft gasifier, Energy Convers. Manage. 42 (2001) 157–172.
[20] I. Petersen, J. Werther, Experimental investigation and modeling of gasification of sewage sludge in the circulating fluidized bed, Chem. Eng. Process. 44 (2005) 717–736.
[21] J.-H. Ferrasse, C. Dumas, N. Roche, Experimental results and model for N-gas compounds production in pure steam gasification for waste water sludge, Chem. Eng. Technol. 34 (2011) 103–110.
[22] B. Groß, C. Eder, P. Grziwa, J. Horst, K. Kimmerle, Energy recovery from sewage sludge by means of fluidised bed gasification, Waste Manage. 28 (2008) 1819–1826.
[23] A. Fuentes, M. Lloréns, J. Sáez, M.I. Aguilar, J.F. Ortuño, V.F. Meseguer, Phytotoxicity and heavy metals speciation of stabilised sewage sludges, J. Hazard. Mater. 108 (2004) 161–169.
[24] P.-C. Hsiau, S.-L. Lo, Extractabilities of heavy metals in chemically-fixed sewage sludges, J. Hazard. Mater. 58 (1998) 73–82.
[25] M. García-Delgado, M.S. Rodríguez-Cruz, L.F. Lorenzo, M. Arienzo, M.J. Sánchez-Martín, Seasonal and time variability of heavy metal content and of its chemical forms in sewage sludges from different wastewater treatment plants, Sci. Total Environ. 382 (2007) 82–92.
[26] M. Pazos, G.M. Kirkelund, L.M. Ottosen, Electrodialytic treatment for metal removal from sewage sludge ash from fluidized bed combustion, J. Hazard. Mater. 176 (2010) 1073–1078.
[27] Council Directive 1999/31/EC of 26 April 1999 on the landfill of waste.
[28] A.A. Zorpas, A.G. Vlyssides, G.A. Zorpas, P.K. Karlis, D. Arapoglou, Impact of thermal treatment on metal in sewage sludge from the Psittalias wastewater treatment plant, Athens, Greece, J. Hazard. Mater. 82 (2001) 291–298.
[29] A. Obrador, M.I. Rico, J.M. Alvarez, J. Novillo, Influence of thermal treatment on sequential extraction and leaching behaviour of trace metals in a contaminated sewage sludge, Bioresour. Technol. 76 (2001) 259–264.
[30] I.H. Hwang, Y. Ouchi, T. Matsuto, Characteristics of leachate from pyrolysis residue of sewage sludge, Chemosphere 68 (2007) 1913–1919.
[31] J.o.R.S.a. Technology, H. Saveyn, J.-H. Ferrasse, A.B. Hernandez, J. Rose, P. Van der Meeren, N. Roche, The distribution of heavy metals following sewage sludge gasification, J. Residuals Sci. Technol. (2011).
[32] R. Richaud, H. Lachas, A.E. Healey, G.P. Reed, J. Haines, K.E. Jarvis, A.A. Herod, D.R. Dugwell, R. Kandiyoti, Trace element analysis of gasification plant samples by I.C.P.-M.S.: validation by comparison of results from two laboratories, Fuel 79 (2000) 1077–1087.
[33] I. Jarvis, K.E. Jarvis, Plasma spectrometry in the earth sciences: techniques, applications and future trends, Chem. Geol. 95 (1992) 1–33.
[34] W. Windig, Spectral data files for self-modeling curve resolution with examples using the SIMPLISMA approach, Chemom. Intell. Lab. Syst. 36 (1997) 3–16.
[35] P. Chaurand, Apport de la cristallochimie et de la spéciation du chrome et du vanadium à la modélisation de l'altération de granulats artificiels (sous-produits d'aciérie), PhD Tesis (2006).
[36] S. Legros, P. Chaurand, J.r.m. Rose, A. Masion, V.r. Briois, J.-H. Ferrasse, H.S. Macary, J.-Y. Bottero, E. Doelsch, Investigation of copper speciation in pig slurry by a multitechnique approach, Environ. Sci. Technol. 44 (2010) 6926–6932.
[37] S. Rio, C. Verwilghen, J. Ramaroson, A. Nzihou, P. Sharrock, Heavy metal vaporization and abatement during thermal treatment of modified wastes, J. Hazard. Mater. 148 (2007) 521–528.
[38] E. Frossard, J.P. Bauer, F. Lothe, Evidence of vivianite in $FeSO_4$-flocculated sludges, Water Res. 31 (1997) 2449–2454.
[39] B.D. Soares, C.E. Hori, C.E.A. Batista, H.M. Henrique, Thermal decomposition and solid characterization of calcium oxide in limestone calcination, in: L. Salgado, F.A. Filho (Eds.), Advanced Powder Technology VI, Trans Tech Publications Ltd., Stafa-Zurich, 2008, pp. 352–357.
[40] S. Gunasekaran, G. Anbalagan, Spectroscopic study of phase transitions in natural calcite mineral, Spectrochim. Acta A-Mol. Biomol. Spectrosc. 69 (2008) 1246–1251.
[41] R.L. Frost, M.L. Weier, W. Martens, J.T. Kloprogge, Z. Ding, Dehydration of synthetic and natural vivianite, Thermochim. Acta 401 (2003) 121–130.
[42] P.L. Tien, T.C. Waugh, Thermal and X-ray studies on earthy vivianite in graneros shale (upper cretaceous), kansas, Am. Mineral. 54 (1969).
[43] C.R. Cheeseman, C.J. Sollars, S. McEntee, Properties, microstructure and leaching of sintered sewage sludge ash, Resour. Conserv. Recycl. 40 (2003) 13–25.
[44] T. Rosenqvist, Principles of Extractive Metallurgy, Tapir Academic Press, 2004.
[45] G.-s. Liu, V. Strezov, J.A. Lucas, L.J. Wibberley, Thermal investigations of direct iron ore reduction with coal, Thermochim. Acta 410 (2004) 133–140.
[46] K.-S. Wang, C.-J. Sun, C.-Y. Liu, Effects of the type of sintering atmosphere on the chromium leachability of thermal-treated municipal solid waste incinerator fly ash, Waste Manage. 21 (2001) 85–91.
[47] D.W. Kirk, C.C.Y. Chan, H. Marsh, Chromium behavior during thermal treatment of MSW fly ash, J. Hazard. Mater. 90 (2002) 39–49.